WATER RESOURCES RESEARCH, VOL. 49, 2701–2713, doi:10.1002/wrcr.20234, 2013

Analytic probability distributions for snow-dominated streamflow

B. Schaefli,[1] A. Rinaldo,[1,2] and G. Botter[2]

Received 18 September 2012; revised 25 March 2013; accepted 28 March 2013; published 28 May 2013.

[1] We propose a novel analytical description of the streamflow probability distribution functions (pdfs) in Alpine catchments characterized by pronounced, snow-dominated winter low flows. Knowledge about such hydrological regimes is crucial for water resources management in mountain environments and the related wide range of socio-economic, environmental and ecological services. We use a stochastic framework, generalizing that employed by Botter et al. (2007b), to link precipitation (rain and snow) and streamflow dynamics. The effect of snow dynamics on the flow regime is specifically included by incorporating the temporary disconnection of high-elevation areas that experience freezing conditions over the entire winter season, and the delay produced on streamflow formation by the temporary accumulation (and later melting) of snow at lower elevations. The novel analytical model employs four parameters that can be directly estimated from observed discharge, precipitation and air temperatures, and one calibration parameter (the elevation threshold z^* delimiting catchment areas with a permanent seasonal snow cover that is nonresponsive during winter owing to snow accumulation without melt). We test the developed model for 14 catchments with contrasting hydroclimatic conditions, located in the Swiss and the Italian Alps. Overall, the proposed analytic model reproduces the observed streamflow pdfs remarkably well. Exceptions exist, though, and the possible origin of deviations between observed and modeled pdfs are discussed. We suggest that our approach marks a progress toward the general statistical characterization of catchment streamflow variability.

Citation: Schaefli, B., A. Rinaldo, and G. Botter (2013), Analytic probability distributions for snow-dominated streamflow, *Water Resour. Res.*, *49*, 2701–2713, doi:10.1002/wrcr.20234.

1. Introduction

[2] Winter streamflow dynamics in mountainous catchments are strongly affected by the accumulation and melting of water in form of snow. In the Swiss Alps for example, above 1000 m a.s.l. more precipitation falls as snow than as rain [*Grünewald et al*., 2010]. This results in a so-called nival or a pluvio-nival streamflow regime with a distinct low-flow period during the winter months and high-summer flows [e.g., *Horton et al*., 2006]. From a hydrological perspective, the effect of snow can be seen as temporally disconnecting part of the catchment from the active streamflow network [*DeBeer and Pomeroy*, 2010; *Tobin et al*., 2013] and as introducing a delay between the moment when water falls as snow and when it is released from the snowpack and contributes to streamflow at the outlet of the catchment. This paper proposes an analytical approach to describe the probability distribution function (pdf) of winter streamflows affected by snow dynamics; the framework is based on the idea that the streamflow variability during winter results from the interplay between the stochastic variability of inputs in terms of timing and amount and the storage capacity of catchments.

[3] As such, this paper represents an extension of the work of *Botter et al*. [2007a, 2007b, 2008], who proposed a similar analytical framework to describe the pdf of daily streamflow triggered by subsurface flow induced by stochastic precipitation forcings. As will become clear later in this paper, the proposed extension is aimed at incorporating (i) the temporary disconnection of high-elevation areas that experience freezing conditions over the entire winter season and (ii) the delaying effect on streamflows produced by the temporary accumulation of snow at lower elevations.

[4] To date, the vast majority of snow-hydrological studies are based on input-output models that simulate snowmelt-influenced streamflow with the help of physics-based snow models or of simplified so-called temperature-index models (see, e.g., *Magnusson et al*., [2011], where the performance of the two approaches are compared for a Swiss catchment). Depending on the required output resolution, these models are either spatially distributed or lumped (for a short discussion, see, e.g., *Perona et al*. [2008]; *Tobin*

Additional supporting information may be found in the online version of this article.

[1]Laboratory of Ecohydrology (ECHO), School of Architecture, Civil and Environmental Engineering (ENAC), Ecole Polytechnique Fédérale de Lausanne, Lausanne, Switzerland.

[2]Dipartimento di Ingenegneria Civile, Edile e Ambientale Università di Padova, Padua, Italy.

Corresponding author: B. Schaefli, Laboratory of Ecohydrology, School of Architecture, Civil and Environmental Engineering (ENAC), Ecole Polytechnique Fédérale e de Lausanne, Station 2, 1015 Lausanne, Switzerland. (bettina.schaefli@epfl.ch)

0043-1397/13/10.1002/wrcr.20234

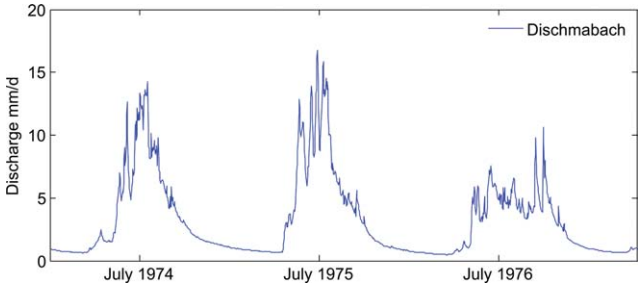

Figure 1. Observed streamflow for the Dischmabach, Switzerland.

et al. [2013]). Existing analytic studies of snow-cover dynamics generally focus on the description of snow depth or snow water equivalent [*Woody et al*., 2009; *Woods*, 2009; *Perona et al*., 2007] to explain e.g. the length of the accumulation period or the location of the end-of-summer snowline (elevation where snow lasts over the entire year). Similarly, *Hantel and Hirtl-Wielke* [2007] proposed a simple analytical model to relate the yearly snow cover duration to temperature. There are only very few analytic descriptions of snow-dominated streamflow dynamics; *Allamano et al*. [2009] studied the temperature-related shift of flood-frequency curves, while *Molini et al*. [2011] proposed a minimalistic model of snow accumulation and melt dynamics to provide an analytic characterization of the annual peak discharge on the basis of the temperature regime.

[5] In the present paper, we focus on the analytical description of winter low flow, as a starting point for the analytic description of entire snow-dominated hydrological regimes. Low flow results from the interplay of snow accumulation and melting in catchments that remain at least partly responsive during winter. The proposed streamflow pdf has four parameters that can be estimated directly from observed precipitation, temperature and discharge time series, and one parameter currently obtained from solving an inverse-problem. Further analyses may explore suitable, measurable proxies. Based on 14 case studies from the Swiss and Italian Alps, we test the ability of the analytical model to reproduce observed winter stream flow pdfs; these case studies cover a sufficiently large range of hydrological regimes and Alpine climates to draw first conclusions on the reliability of the model and the estimated parameter values.

[6] The remainder of the paper is organized as follows: Section 2 presents the derivation of the analytic winter streamflow pdfs, followed by a description of the case studies (section 3) and a detailed comparison of the modeled and observed streamflow pdfs (section 4). The relevance of the proposed approach is discussed in detail in section 5 before summarizing the main conclusions (section 6).

2. Methods

2.1. Alpine Winter Flow

[7] Snowfall and melt are both strongly driven by temperature and other energy balance components (e.g., radiation) that show strong spatial (and in particular altitudinal) gradients [*Jabot et al*., 2012; *Tobin et al*., 2013]. Accordingly, freezing and melting conditions might prevail simultaneously, but at different locations, within a given catchment, implying that some locations experience snowfall and accumulation on the ground, while others contribute input to streamflow through snowmelt and rainfall.

[8] On average, considered over an entire winter period, a catchment can thus be conceptually divided into three zones: Zone I is characterized by occasional snowfall and does not build up a significant snowpack lasting more than a few days. This region is unaffected by snow dynamics during the winter. Zone II is characterized by regular snowfall events, which are however followed by (more or less sporadic) periods with enhanced snowmelt. In this zone, one or several significant snowpacks build up during the winter season but are assumed to be almost completely depleted during the same season. This can be thought of as the portion of the catchment which is actively contributing to streamflow during the winter. Zone III corresponds to the area where all precipitation falls as snow and where the snowpack lasts the entire winter. This last zone does not contribute significantly to streamflow during the winter, i.e., it corresponds to the nonresponsive area.

[9] There might also be zones where the snowpack lasts over several seasons and contributes to the buildup of permanent snow (firn) and ice. In this study, coherently with the aims of the work, such glacier-covered areas are removed from the considered catchments.

[10] In the following, we discuss how the model of *Botter et al*. [2007b] can be extended to describe the winter streamflow pdf of catchments that are mainly composed of zones 2 and 3, i.e., of catchments that are strongly influenced by snow accumulation but that nevertheless release some water during the winter period. Such catchments will show a pronounced winter low-flow regime without significant peaks (see, e.g., Figure 1).

2.2. Analytic Winter Streamflow pdf

[11] The basis of the model of *Botter et al*. [2007b] is a stochastic description of daily streamflow dynamics, which are assumed to result from the superposition of a sequence of subsurface water flow impulses triggered by precipitation. In particular, the sequence of streamflow-producing rainfall events is assumed to be a subset of the overall rainfall. This subset is composed of the events bringing enough water to fill the water deficit created by plant transpiration in the root zone, and drive the soil water content in this region above its retention capacity. Therefore, such pulses determine an excess of water in the root zone, which is eliminated through the subsurface hydrologic response of the catchment. If the subsurface storage of the catchment is assumed to behave like a linear reservoir, each pulse determines a sudden increase of the streamflow, which is followed by an exponential-like recession.

[12] In mathematical terms, a pulse with an excess volume $V_i\,[\mathrm{L}^3]$ released at time t_i from the root zone provides a contribution to the overall streamflow which is $V_i k \exp[-k(t-t_i)]$, where $k\,[\mathrm{T}^{-1}]$ represents both the recession rate and the inverse of the mean response time of the exponential hydrograph. Hence, the instantaneous streamflow increment determined by the above water flow impulse at the time when the pulse is produced from the

root zone (i.e., for $t = t_i$) is $V_i k$ (i.e., k times the volume of the pulse). Provided that the system is linear, the overall streamflow is just the sum of the contribution of the different effective pulses taking place.

[13] According to the above assumptions, the stochastic dynamical equation for Q at a daily timescale is:

$$\frac{\mathrm{d}Q(t)}{\mathrm{d}t} = -kQ(t) + \xi_t, \tag{1}$$

where the first term at the right-hand side expresses the exponential decay of the flow Q in between the events, and the second term ($\xi_t \left[\mathrm{L}^3/\mathrm{T}^2\right]$) formally imbeds the series of stochastic jumps induced on Q by the sequence of streamflow producing rainfall events.

[14] If the overall rainfall forcing is modeled as a marked Poisson process with frequency λ_P and exponentially distributed precipitation depths with average α [*Rodriguez-Iturbe et al*., 1999; *Rodriguez-Iturbe and Porporato*, 2004], and under some additional assumptions on soil moisture dynamics [*Botter et al*., 2007a, 2007b, 2008], the term ξ_t in equation (1) can be shown to be well approximated by a Poisson process similar to that mimicking the main rainfall, but characterized by a reduced frequency λ. In practice, this means that the streamflow-producing events have an instantaneous duration (i.e., ξ_t is different from zero only during a set of finite times), producing a sequence of localized jumps in the streamflow Q. According to the Poissonian nature of the process, the interarrival times between these jumps are exponentially distributed with mean $1/\lambda$.

[15] Given the exponential distribution of the rainfall depths, the sequence of excess volumes released from the root zone is also exponentially distributed, with mean $A\alpha$ (A being the overall catchment area, transforming depths into volumes). Accordingly, the extent of the jumps experienced by Q are random and exponentially distributed with mean $kA\alpha$ (k times the pulse volume, see discussion above).

[16] The resulting streamflow pdf associated to the process defined by equation (1) reads as [*Botter et al*., 2007b, equation (16)]:

$$p(Q, t \to \infty) = \frac{1}{\Gamma\left(\frac{\lambda}{k}\right)} \frac{1}{Q} \left(\frac{Q}{\alpha k A}\right)^{\frac{\lambda}{k}} \exp\left(-\frac{Q}{\alpha k A}\right), \tag{2}$$

[17] Γ being the (complete) Gamma function.

[18] In the general rain-fed case, λ is related to precipitation and soil moisture parameters [*Botter et al*., 2007b, equation (6)]. Here it can be assumed that during winter, there is no soil moisture loss through transpiration and that the soil moisture remains permanently close to its retention threshold. It follows that all precipitation events trigger subsurface flow and, accordingly, streamflow-producing precipitation events can be described as a Poisson process with the same frequency of the precipitation process, i.e., $\lambda = \lambda_P$.

[19] To this stage, the derivation did not take into account the fact that in snow-influenced environments, part of the precipitation falls as snow. The basic idea underlying the remaining steps is that the winter low-flow regime results from a smoothing of the incoming precipitation pulses through the temporary accumulation of snow in the catchment parts that remain responsive during the winter period (zone II). We assume that this effect can be modeled by introducing a delay in the catchment response time:

$$\tau_w = \tau_k + \tau_D, \tag{3}$$

where $\tau_k = k^{-1}$ [T] is the mean catchment response time in absence of snow, τ_D [T] is the delay in the catchment residence time caused by temporary accumulation of snow and τ_w [T] is the resulting mean response time during winter.

[20] The residence time delay incorporates two effects: (i) the average length of periods when all water is trapped in the snowpack (i.e., when the snowpack is in freezing conditions) and (ii) the delaying effect caused by the fact that any snowmelt or rain water has to travel through the snowpack before entering the subsurface travel paths to the catchment outlet. Given that zone II is assumed to have one or several temporary snowpacks during the winter (and not a single, important seasonal snowpack as zone III), the time scale of this traveling within the snowpack can be assumed to be much shorter than the freezing time scale (which will typically be of the order of magnitude of days). Accordingly, it will be assumed that τ_D can be estimated as a function of the freezing regime (to be further discussed in section 2.3).

[21] Given that a part A^* of the catchment is effectively "dormant" or nonresponsive during the winter (only snow accumulation, no melt), the catchment area in equation (2) has to be replaced by the responsive area, $A - A^*$.

[22] The final winter streamflow pdf in presence of snow reads as

$$p(Q, t \to \infty) = \frac{1}{\Gamma\left(\frac{\lambda_P}{k_w}\right)} \frac{1}{Q} \left[\frac{Q}{\alpha k_w (A - A^*)}\right]^{\frac{\lambda_P}{k_w}} \exp\left[-\frac{Q}{\alpha k_w (A - A^*)}\right], \tag{4}$$

where $k_w = \tau_w^{-1}$.

[23] The nonresponsive catchment parts can be assumed to be the ones where during the entire winter, on average, the snow melting is negligible with respect to the accumulation. An exact description of A^* would require a detailed analysis of all components of the energy balance [e.g., *Lehning et al*., 2006]. It is well known, however, that temperature is a very good proxy for the dominant components of the energy balance [*Ohmura*, 2001], which explains the success of so-called temperature-index snow melt models [e.g., *Hock*, 2003; *Zappa et al*., 2003; *Schaefli et al*., 2005]. Given, furthermore, that on average over an entire winter period, temperature shows a strong altitudinal gradient, we assume that we can reasonably discriminate the responsive part from the nonresponsive part of the catchment based on a threshold altitude z^*, i.e., $A^* = AP(Z > z^*)$ where $P(Z > z^*)$ represents the probability that the altitude Z is higher than the threshold altitude z^*, which can be estimated from the hypsographic curve of a given catchment. This assumption only holds for catchments that include areas that are low enough to experience melting conditions (i.e., temperature above 0°C) during the winter season.

Table 1. Model Parameters: Units, Meaning, Estimation Method and Effect of an Increase of This Parameter Value on Streamflow pdf in Terms of Mean Streamflow, $\langle Q \rangle$, and pdf Peak Value, pdf_m, where +(+) Stands for a (Strong) Increase, −(−) for a (Strong) Decrease and 0 for No Effect

Symbol	Unit	Meaning	Estimation	$\langle Q \rangle$	pdf_m
α	mm	Mean daily precipitation depth	Observed daily precipitation	++	−
γ'_P	mm^{-1}	Precipitation distribution parameter	$\gamma'_P = \alpha^{-1}$	−	++
λ_P	T^{-1}	Precipitation frequency	Observed daily precipitation	++	−
τ_k	T	Residence time in absence of snow	Observed summer streamflow	0	+
τ_D	T	Residence time delay due to snow	Observed winter temperature	0	+
z^*	m	Altitude threshold	Calibration on obs. streamflow pdf	++	−
A	km^2	Catchment area	Topographic map	0	0
A^*	km^2	Nonresponsive area	$A^* = f(z^* \vert \text{hypsographic curve})$	−	++

[24] This represents, of course, a crude simplification of the high-spatial heterogeneity of snow distribution in complex terrain [e.g., *Lehning et al*., 2011; *Clark et al*., 2011]. However, modeling of the hydrologic response in snow-dominated environments based on elevation bands has been shown to yield good results for daily time steps at the catchment scale [e.g., *Schaefli et al*., 2005; *Stahl et al*., 2008].

[25] It is noteworthy that this division of the catchment into a responsive and a nonresponsive catchment part is assumed to reflect the integrated average winter conditions in the catchment and is estimated from the hydrologic response (see following section). In other words, the responsive catchment part is inferred after confronting the model with observed hydrologic data and not a priori based only on the temperature regime as in the work of *Allamano et al*. [2009] on alpine flood risk.

2.3. Parameter Estimation

[26] The streamflow pdf for winter low flow has five parameters to be estimated (Table 1) from observed time series: the frequency of precipitation events, λ_P, the mean precipitation α, the residence time τ_k, the increase of residence time due to snow accumulation, τ_D and the altitudinal limit between the responsive and the nonresponsive catchment part, z^*. This last parameter is the only calibration parameter; once all other parameters are estimated from observed data (see hereafter), z^* is adjusted with a systematic search (i.e., testing all possible z^* values) such as to minimize the bias between the pdf obtained from observed streamflow (called observed pdf from here on) and the analytical pdf (equation (4)).

[27] The precipitation parameters are estimated directly from the reference precipitation series for a given catchment; λ_P is estimated as the average number of precipitation events (each day with precipitation is an event) occurring over the reference observation period. α is estimated as the average amount of precipitation on days with precipitation [*Rodriguez-Iturbe and Porporato*, 2004].

[28] The recession rate k, which defines the mean residence time in the catchment in absence of snow, is estimated with the classical Brutsaert-Nieber recession analysis [*Brutsaert and Nieber*, 1977] for recession events occurring during summer months (when snowmelt is assumed to have no influence) [e.g., *Ceola et al*., 2010; *Botter et al*., 2007a]. These events are identified using all summer streamflow data points lying below the 90% quantile of the summer streamflow pdf as threshold. Such a threshold-based selection approach ensures a simple automatic selection of recession events for all catchments.

[29] The key parameter τ_D is estimated based on the length of periods showing freezing conditions when incoming precipitation falls as snow and accumulates on the ground and no snowmelt occurs. The definition of such conditions is complex given that the precipitation phase will depend on the atmospheric conditions where precipitation is formed as well as on the near-ground conditions [*Bourgouin*, 2000; *Tobin et al*., 2012] and that snowmelt depends on the local energy balance. As mentioned previously, temperature is a good proxy for dominant melt drivers and it can be assumed that melt occurs if air temperature rises above 0°C. For the precipitation phase, it is generally observed that snowfall can also occur at temperatures above 0°C [*Rohrer et al*., 1994], in a transition interval of a few degrees, depending namely on the relative humidity. For the purpose of the model, the assumption of a 0°C threshold for precipitation phase and melt has been chosen. Different choices have a weak impact on the results.

[30] Accordingly, τ_D is estimated as the mean duration of periods with temperature below 0°C. τ_D can be estimated directly from observed temperature series by computing the average length of freezing periods. Table 1 summarizes all model parameters, their estimation method as well as their effect on the streamflow pdf shape.

2.4. Summary of Assumptions

[31] The applicability of the main assumptions introduced in this study is briefly discussed hereafter. For an in-depth discussion of the assumptions underlying the analytic framework, the reader is referred to *Botter et al*. [2008] for a general summary, to *Rodriguez-Iturbe et al*. [1984, 1999] and *Rodriguez-Iturbe and Porporato* [2004] for the Poisson assumption for rainfall, to *Rodriguez-Iturbe et al*. [1999]; *Settin et al*. [2007]; and *Laio et al*. [2001] for a discussion of soil moisture dynamics and to *Botter* [2010] for the behavior of recessions.

[32] We would like to emphasize again here that the key advantage of the Poisson assumption for precipitation relies in the simplicity of the scheme, the ease of application, and the direct measurability of the parameters (frequency of arrival, mean intensity) from appropriate databases. We checked that the assumption of exponentially distributed precipitation depths holds for summer as well as for winter precipitation for all case studies (see an example in Figure 4).

[33] Next, the analytic pdf assumes that all incoming precipitation transits through the subsurface, i.e., everything infiltrates. In the presence of snow and of progressive melting of the snow cover, this assumption will generally hold, except in two situations: (i) If the soil experiences significant freezing prior to the development of a snowpack, its infiltration capacity might be considerably reduced. *Bayard et al*. [2005] found for their study sites in the Swiss Alps that 25%–35% of snowmelt water ran off laterally during a winter with a very shallow snow pack. (ii) Significant lateral runoff on the snow/soil interface can also occur in the case of exceptionally strong melting events triggered for example by rain-on-snow [*Marks et al*., 1998]. Both types of situation would lead to visible streamflow peaks during the winter low-flow period, but they are assumed to be exceptional for hydrological regimes with a pronounced winter low flow and will not influence the general shape of the winter streamflow pdf.

[34] With this respect, it is important to distinguish the term "responsive catchment part" from what is sometimes called the "rain-snow transition zone" [*Marks et al*., 1998]; this last term typically applies to low-elevation areas where snowpacks are very shallow and where the entire snowpack melts regularly during single rainfall events. Such areas will show regular streamflow peaks during the winter (e.g., *Marks et al*. [1998] locates this zone around 300–1000 m asl. for the Pacific Northwest). The proposed approach, however, applies to catchments that are located at sufficiently high altitudes such as to show no significant streamflow peaks during the winter (see an example from the Swiss Alps in Figure 1), but that have a pronounced winter low flow. In the Alps, the occurrence of such a nival regime can be assumed to occur for catchments with mean elevation above around 1500 m asl. [*Viviroli and Weingartner*, 2004].

[35] In other regions, other climatic factors might come into play but there will still be zones showing this typical nival regime [e.g., *Hannah et al*., 2005, for the Himalaya]. However, the model will only apply if this nival regime results from the interplay of responsive areas and of catchment areas that accumulate all incoming precipitation during the entire winter period. This might typically not be the case in the Himalaya where the accumulation and the melt period coincide [e.g., *Kaser et al*., 2010].

3. Case Studies

[36] Two sets of case studies are used to illustrate the ability of the analytical pdf to reproduce observed winter stream pdfs: (i) a set of subcatchments of the Italian Piave river (Veneto region) and ii) a collection of catchments of the Swiss Alps. These two sets of catchments cover different Alpine climates as well as a range of different catchment sizes; this allows to thoroughly test the model's ability to reproduce observed winter streamflow pdfs and gives first insights into possible regional relationships of the model parameters.

3.1. Italian Catchments

[37] The Piave river basin is one of the most important Alpine catchments of North–Eastern Italy with a size of around 4200 km^2 and a main reach length of 220 km. The highest point of the catchment is Monte Peralba (2694 m asl.). It has a continental-temperate, rather humid climate, which is typical for the Southern Alps. The rainfall regime is of the so-called subcoastal-alpine type with annual rainfall of between 1400 and 1700 mm depending on the location; it presents two peaks of precipitation during spring and fall. Winter (December-February) is the driest season of the year; the driest month is July. The coldest temperatures are observed in February, with frequent snowfall during the winter in the higher parts of the catchments. Further details on the catchment morphology and hydrology can be found in *Botter et al*. [2010].

[38] The hydrological regime of the Piave river basin is strongly influenced by numerous water works. This study considers seven undisturbed headwater catchments in the mountain part of the basin (see Figure 2 and Table 2). Their sizes range from around 10 to 350 km^2; some of them are nested (Figure 2). None of these catchments has significant glaciers. The available meteorological stations for precipitation and temperature data, all located within the Piave river catchment are listed in Tables 2 and 4 (only stations with more than 10 years of observation). For the cases where several precipitation stations are available for a catchment, the precipitation parameters are estimated as the mean of the parameters obtained for each series. As preliminary analyses showed, no significant model performance improvement could be obtained with an area-weighted approach for precipitation interpolation. For temperature, all available series for a given catchment are averaged before parameter estimation.

3.2. Swiss Catchments

[39] We selected seven undisturbed headwater catchments for which there are good discharge observations and that are representative of all hydro-climatic regions of Switzerland, north and south of the main ridge of the Alps (Figure 3). The selected catchments have mean elevations of between 1500 and 3000 m a.s.l. (Table 3). Their hydrological regimes differ strongly, depending on the altitude and on whether they are north or south of the Alps (see *Horton et al*. [2006], for an illustration of the regimes), with namely much higher annual rainfall south of the Alps. As for the Italian case studies, simple averaging is used to obtain the reference meteorological series for catchments with several stations (see Table 4).

[40] All catchments are all strongly snow-influenced and have a pronounced winter low-flow period from December to February. Their non glacier-covered catchment areas range from 14 to 65 km^2. The hypsographic curve for the identification of the responsive area as a function of the threshold altitude z^* is based on the digital elevation model of Switzerland of a horizontal resolution of 25 m [*SwissTopo*, 2005]. Glacier-covered areas are identified based on the digital landscape model of Switzerland [*SwissTopo*, 2008] and removed from the hypsographic curves.

4. Results

4.1. Estimated Parameters

[41] All parameter values (see Table 5) are estimated according to the methods outlined in section 2.3 for the

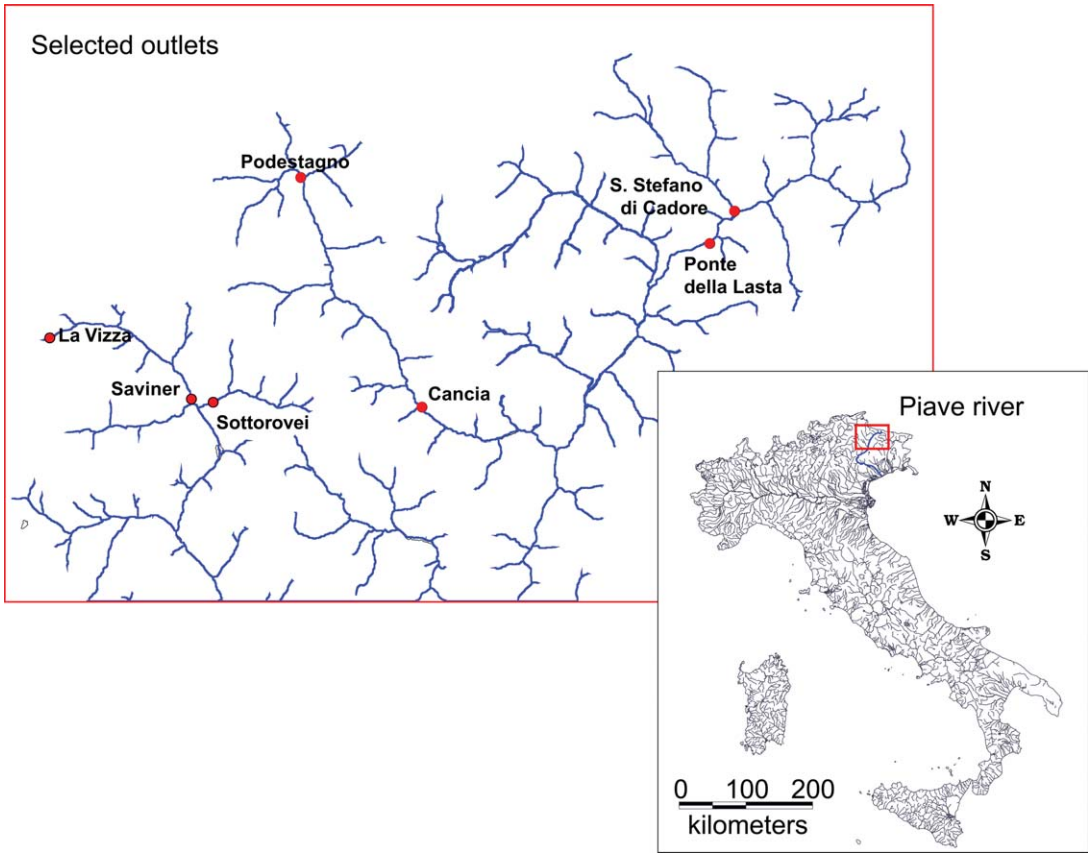

Figure 2. The location of the Italian case studies within the Piave basin and its location within Italy [Source: *The Geocommunity*, 2013].

observation periods indicated in Tables 2 and 3. The winter period for the estimation of γ_p, λ_P, τ_D, and z^* is defined for all catchments as December-February since these are the coldest months in this climate. The implications of the choice of this period are further discussed in section 5. The summer period for the estimation of τ_k is defined as

Table 2. Italian Catchments With Mean Altitude, Catchment Area, Used Streamflow Observation Period and Mean Winter Discharge $\langle Q_w \rangle$ (the Name of the Outlet Is Indicated for Rivers With Several Gauges)

Name	Abbreviation	Observed Period	Area (km^2)	Altitude (m a.s.l.)	$\langle Q_w \rangle$ (mm d^{-1})
Fiorentina (Sottovorei)	Sot	1993–2007	58.2	1840	1.1
Cordevole (La Vizza)	Lav	1984–2007	7.8	2184	0.6
Cordevole (Saviner)	Sav	1990–2007	109.3	1906	0.9
Boite (Podestagno)	Pod	1992–2007	82.4	2183	0.9
Boite (Cancia)	Can	1986–2007	314.2	1855	1.3
Padola (S. Stefano)	Ste	1986–2007	130.4	1721	1.3
Piave (Ponte della Lasta)	Pdl	1989–2006	355.0	1670	1.4

Table 3. Swiss Catchments With Catchment Area, Mean Altitude, Mean Winter Discharge $\langle Q_w \rangle$ and Glacier Coverage [*Swiss Federal Office for the Environment*, 2009][a]

Name	Abbreviation	Observed Period	Area (km^2)	Altitude (m a.s.l.)	Glacier (%)	$\langle Q_w \rangle$ (mm d^{-1})
Dischmabach	Dis	1974–2010	43.3	2732	2.1	0.9
Krummbach	Kru	1974–2010	19.8	2276	3.0	0.8
Massa	Mas	1974–2009	66.5	2668	0*	0.6
Ova da Cluozza	Ova	1974–2009	26.9	2368	2.2	0.7
Poschiavino	Pos	1974–2009	14.1	2283	0.4	1.2
Rein de Sumvitg	Rei	1978–2009	21.8	2450	6.7	1.0
Riale di Calneggia	Ria	1978–2009	24.0	1996	0	1.0

[a]For Massa: size and mean altitude of the nonglacier covered part.

Table 4. Meteorological Stations Used for the Italian and the Swiss Case Studies With The Observed Variable (Precipitation, *P*, or Temperature *T*), the Mean Altitude, the Corresponding Catchments and the Distance to the Catchment (0 Indicates That the Station is Located Within the Catchment)

Name	Variable	Altitude (m a.s.l.)	Catchment	Distance (km)
Arabba	*P*, *T*	1648	Sav	0
Caprile	*P*, *T*	1008	Sot	0
Casamazzagno	*P*, *T*	1345	Ste, Pdl	0
Cimacanale	*P*, *T*	1250	Pdl	0
Costalta	*P*, *T*	1240	Pdl	0
Faloria	*P*, *T*	2239	Can	0
Malga Campobon	*P*, *T*	1465	Pdl	0
Passo Falzarego	*P*, *T*	2115	Sot, Sav	0
Passo Monte Croce Comelico	*P*, *T*	1628	Ste, Pdl	0
Passo Pordoi	*P*, *T*	2142	Lav, Sav	0
Podestagno	*P*, *T*	1320	Pod	0
S. Stefano di Cadore	*T*, *P*	895	Pdl	0.5
Passo del Bernina	*P*, *T*	2307	Pos	3.7
Brig	*P*, *T*	666	Mas	8.8
Buffalora	*P*, *T*	1968	Ova	12.5
Cavaglia	*P*	1706	Pos	4.2
Davos	*P*, *T*	1594	Dis	4.9
Matro	*T*	2171	Rei	27.1
Naluns	*T*	2400	Ova	17.6
Robiei	*P*, *T*	1894	Ria	5.6
Simplon-Dorf	*P*, *T*	1495	Kru	5.4
Ulrichen	*P*, *T*	1345	Mas,Kru	26.6,38.4
Vrin	*P*, *T*	1458	Rei	8.5
Weissfluhjoch	*P*, *T*	2690	Dis	8.4
Zernez	*P*	1471	Ova	2.3

June-August, which is assumed to be a period that is mostly snow-free and hence the streamflow recession not influenced by snowmelt.

[42] The precipitation parameters α and λ_P are estimated from the reference precipitation series (either form a single station or averaged from several stations, see section 3).

[43] The reference precipitation series do not necessarily reflect the catchment average conditions. The frequency λ_P shows low variability among stations in a given hydro-climatic region. For the 64 automatic Swiss weather stations recording since 1982 (the so-called ANETZ stations, *Suter et al*. [2006]), the average frequency of rainfall events varies between 0.28 and 0.49 d^{-1} with a standard deviation of 0.05 d^{-1}. The annual precipitation amount, however, may show strongly variable gradients [*Sevruk*, 1997]. *Tobin et al*. [2011] report for the Viege catchment, a neighboring catchment of the Massa catchment (both are part of the Swiss Rhone catchment), mean annual precipitation of around 600 mm at the valley bottom (500 m asl.), 800 mm at 1600 m asl. and more than 2800 mm at altitudes exceeding 4000 m asl.

[44] Given that the model has a calibration parameter, z^*, which directly influences the mean of the pdf, any deviation between the reference and the area-average precipitation amount might be compensated. This compensation effect probably explains the strong inverse relation between α and $A - A^*$ for the Swiss catchments (Figure 5). For the Italian catchments, such a relation between α and $A - A^*$ is not apparent; for these case studies, the available meteorological stations are located within (or very close to) the catchments and can be assumed to be much more representative of the actual area-average precipitation.

[45] Similar to precipitation, the temperature series might also not reflect average conditions in the, a priori unknown, responsive part of the catchment. Given that temperature stations located at different altitudes generally show a clear, albeit time-varying temperature gradient [e.g., *Tobin et al*., 2011], it could be tempting to interpolate, a posteriori, the reference series to the mean altitude of the responsive area (implying an iterative re-estimation of τ_D and z^*). This would require an in-depth analysis of distributed temperature and would restrict the applicability of the methods to areas with a sufficiently dense meteorological network. To keep the model as simple as possible, τ_D is estimated directly from the reference temperature series for the winter period (obtained from one or several stations, see section 3).

[46] The plot of τ_D estimated from observed time series against the mean winter temperature for all analyzed case studies (Figure 6) shows an approximately exponential relationship between mean winter temperature and τ_D, i.e., that mean winter temperature is a good predictor of τ_D for the analyzed region. This plot furthermore suggests that for the majority of case studies of this paper (with mean winter temperature between −2.5°C and −5°C), the value of τ_D

Table 5. Values of the Model Parameters for All Case Study Catchments; the Mean Winter Temperature of the Reference Series, T_w, is Given for Comparison Purposes

Catchment	γ'_P (cm^{-1})	α (mm)	λ_P (d^{-1})	τ_k (h)	τ_D (h)	z^* (m a.s.l.)	A (km^2)	$A - A^*$ (km^2)	rel_{A-A^*}(%)	T_w (°C)
Sot	1.80	5.6	0.23	193	263	1123	**58.2**	48.5	83.4	−3.3
Lav	2.77	3.6	0.27	180	361	1675	7.8	4.8	61.7	−5.0
Sav	2.20	4.5	0.26	278	295	1146	109.3	86.0	78.7	−4.0
Pod	1.73	5.8	0.23	128	248	1376	82.4	56.9	69.1	−3.0
Can	2.06	4.8	0.22	224	323	983	314.2	314.2	100.0	−4.9
Ste	2.17	4.6	0.24	283	283	1005	130.4	130.4	100.0	−3.1
Pdl	2.06	4.8	0.22	178	337	955	355.0	355.0	100.0	−3.7
Dis	1.63	6.2	0.41	179	566	2290	43.3	15.6	36.1	−6.1
Kru	1.28	7.8	0.36	217	309	2090	19.8	6.0	30.3	−3.9
Mas	1.23	8.1	0.33	193	423	2306	66.5	14.0	21.0	−6.4
Ova	2.18	4.6	0.29	113	901	2379	26.9	13.5	50.0	−7.2
Pos	0.90	11.1	0.27	187	876	2206	14.1	5.6	40.0	−6.7
Rei	1.72	5.8	0.30	114	268	2526	21.8	13.1	60.3	−4.1
Ria	0.94	10.6	0.40	146	229	1636	24.0	5.3	22.1	−3.2

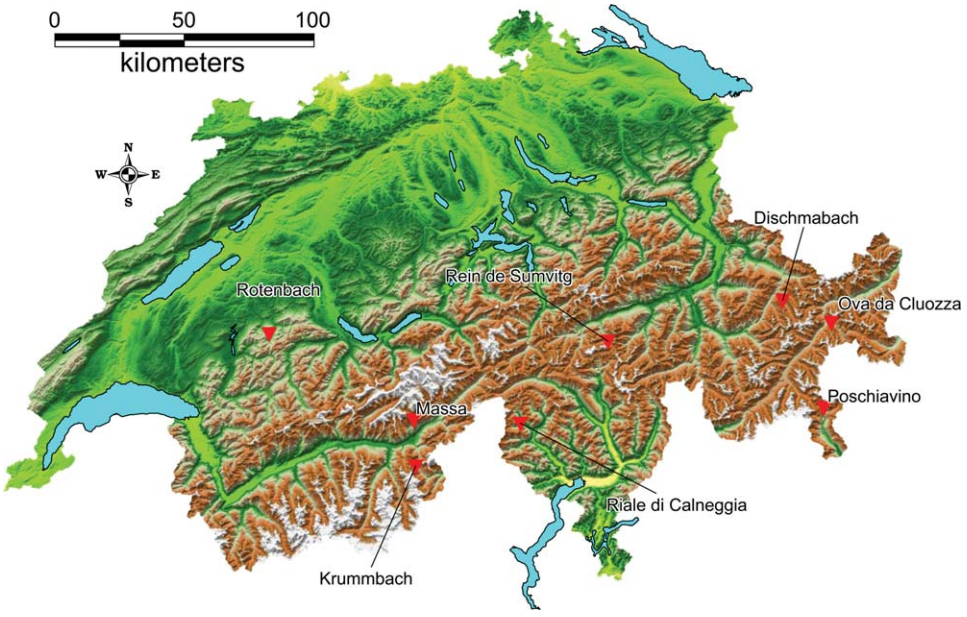

Figure 3. The location of the Swiss case studies within Switzerland [Source: *SwissTopo*, 2008, 2005].

would vary by a few days if the reference temperature time series came from a slightly higher or lower location (with slighter warmer or colder temperatures).

[47] Overall, the estimated values of τ_D for the selected case studies vary from 10 to 38 days, compared to a range of 5–12 days for τ_k (Table 5), which contributes between 11% and 50% of the total winter residence time, with an average of 34%. Given the relatively small sample size (14 catchments), no spatial pattern of τ_k or τ_k/τ_D can be detected.

4.2. Model Performance

[48] The performance of the model for the selected catchments is assessed qualitatively and quantitatively. The

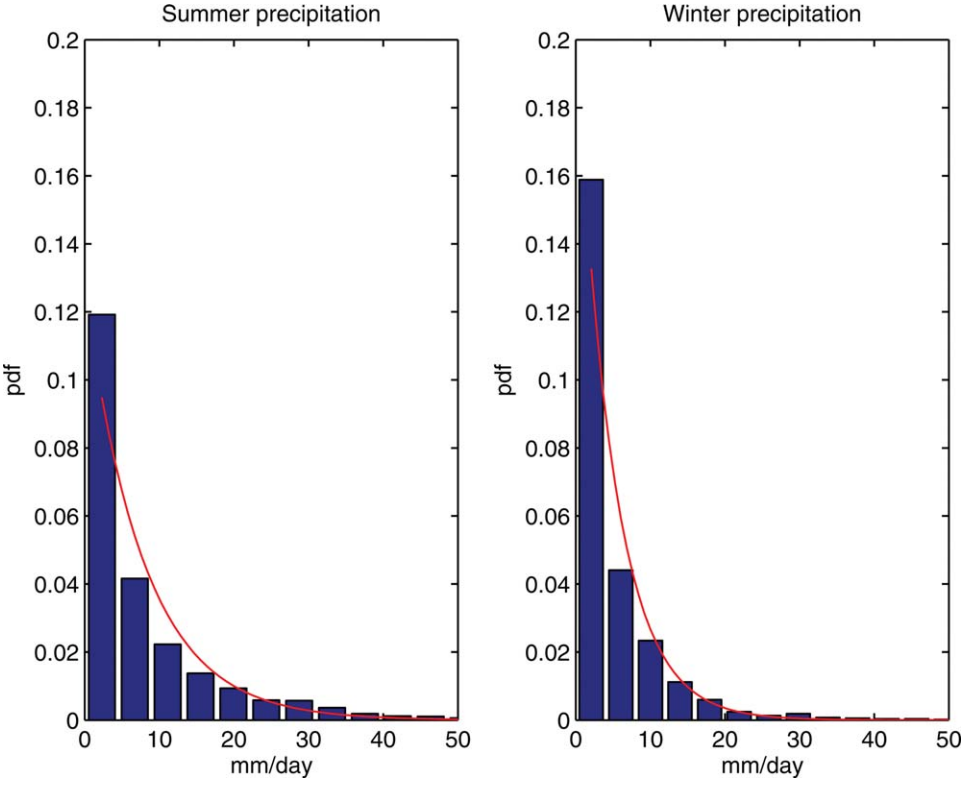

Figure 4. Distribution of observed precipitation depths for the Davos station (Dischma case) study (bars) and fitted exponential distribution (line) for winter and summer precipitation.

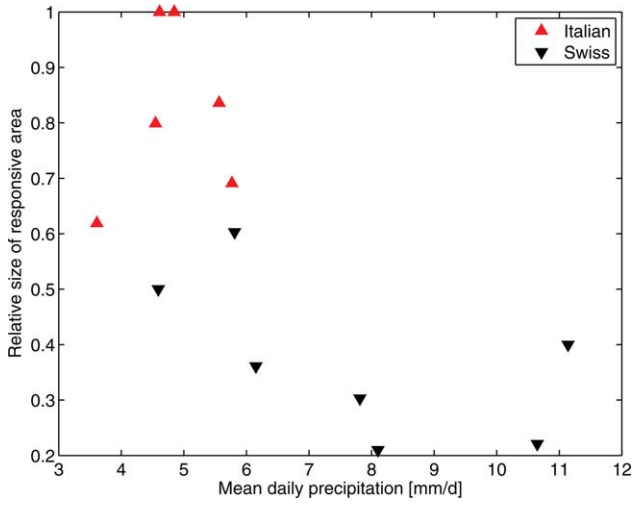

Figure 5. Relation between the mean daily precipitation and the relative size of the responsive area for the Swiss and the Italian catchments (the case studies Can and Pdl fall onto the same point, see Table 5).

qualitative assessment is based on visual inspection and judges whether the model captures the mode of the observed pdf (its value and its location) and whether it captures its general shape. The quantitative evaluation assesses the closeness to the volume of the observed pdf in terms of the relative bias between the two and the Kolmogorov-Smirnov distance between the observed and the modeled pdf (to compare the goodness of fit between the catchments). In addition, we completed a Pearson chi-square goodness-of-fit test [e.g., *Lehmann and Romano*, 2005] with the null hypothesis that the observed winter discharge samples come from the identified analytical pdfs. The underlying Pearson statistics is computed based on the squared and normalized distance between the expected number of samples falling into 15 discharge bins for the model and the observed data. The test is completed assuming that the analytical distribution has two parameters to estimate (the five model parameters combine in fact into a shape and a location parameter of the pdf). The null hypothesis cannot be rejected for any of the case studies.

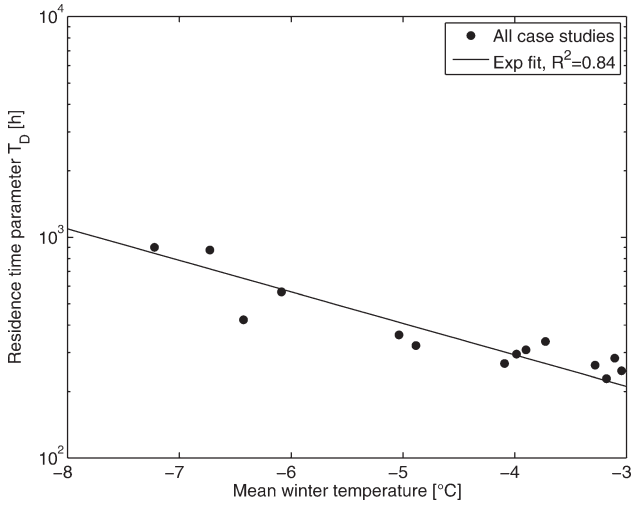

Figure 6. Semilog plot of the estimated response time τ_D against mean winter temperature.

Table 6. Qualitative and Quantitative Comparison of Simulated and Observed Mean Winter Stream Flow pdfs[a]

Catchment	Peak Value	Mode Location	K-S Distance	Bias
Sot	Too low	Ok	0.06	0.0
Lav	Too low	Ok	0.06	0.0
Sav	Too low	Ok	0.11	0.0
Pod	Too low	Slight left	0.14	0.0
Can	Too low	Left	0.25	−16.6
Ste	Too low	Slight left	0.15	−13.6
Pdl	Ok	Slight left	0.24	−23.2
Dis	Too low	Ok	0.04	0.0
Kru	Too low	Ok	0.06	0.1
Mas	Too low	Ok	0.11	0.1
Ova	Too low	Ok	0.05	−0.1
Pos	Too low	Ok	0.04	−0.1
Rei	Too low	Ok	0.09	0.1
Ria	Ok	Ok	0.07	0.1

[a]Bias is indicated in %, K-S stands for Kolmogorov-Smirnov distance.

[49] All results are summarized in Table 6. Overall, the proposed model and the parameters, estimated from the reference meteorological series without any further spatial interpolation, captures the observed streamflow pdfs well, suggesting the robustness of the developed approach (see 4 examples in Figures 7 and 8 and the remaining case studies in Figures S1 and S2 of the supplementary material). All the streamflow pdfs appear to be hump-shaped, with a relatively small mean and a huge peak.

[50] Given that the bias is used as an objective function for the estimation of z^*, its value is generally very low (Table 6), except for the three Italian gauging stations for which the calibrated responsive area is 100%. For Boite at Cancia (Can) and the Piave at Ponte della Lasta (Pdl) this might at least partly be due to observational inconsistencies; in fact, for these two case studies, the observed mean winter discharge is for almost all years higher than the mean winter precipitation. Accordingly, it is probable that either the total winter precipitation input is underestimated or the winter discharge measurement overestimates the actual winter flow.

[51] The location of the mode of the modeled pdf is well captured for most catchments. This indicates that the bias is an efficient objective function for the calibration of z^*. The almost consist underestimation of the mode is related to a rough estimate of the delayed residence time τ_w. This could of course result from the recession parameter τ_k, especially for highly glacierized catchments, where melt of permanent snow and ice might lead to estimates of τ_k which are not representative for the catchment average behavior. In general, however, the delay parameter τ_D, which, as discussed previously, is sensitive to the specific temperature dataset used for estimation, might be considered as being more uncertain. In particular, it can be assumed that the available meteorological stations underestimate the average temperature conditions in the responsive area since, with very few exceptions, the meteorological stations are located at lower elevations. The related underestimation of τ_D might thus explain the underestimation of the observed pdf peaks. Of course, τ_D is also sensitive to the assumption that air

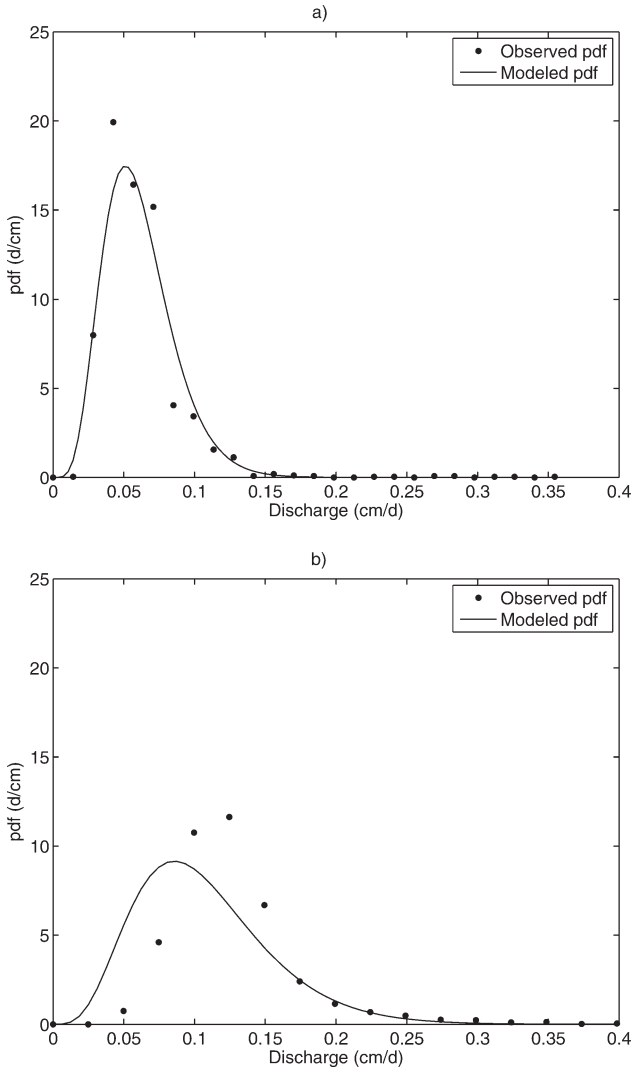

Figure 7. Analytical and observed winter streamflow pdfs for two Italian case studies representing different catchment sizes, elevation ranges and hydrological regimes: (a) Cordevole—La Vizza, (b) Boite—Cancia.

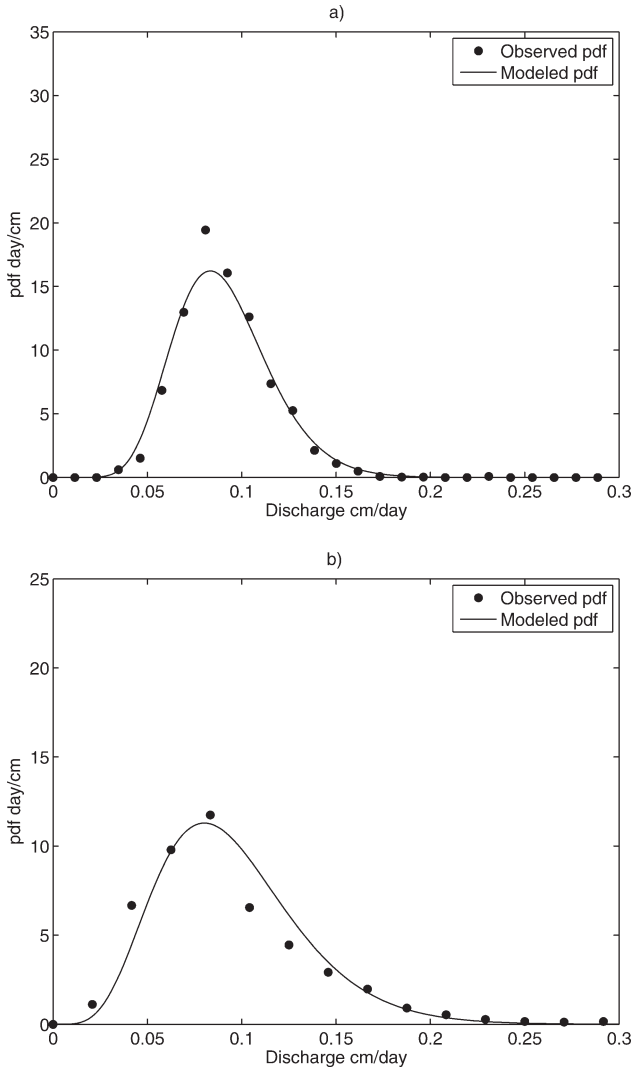

Figure 8. As Figure 7 but for two Swiss case studies: (a) Dischmabach, (b) Riale del Calneggia.

temperature can be used as a proxy to assess average freezing conditions within the snowpack.

[52] The calibrated z^* values range from 1000 to 2500 m asl. Given that this is the only calibration parameter, one might be interested in its physical relevance. A first important test is an analysis of the relationship between z^* and air temperature, which is the main driver of snow accumulation. A strong inverse relationship might be expected. Figure 9 shows, however, a large spread, which can be attributed to the fact that the temperature series have not been interpolated to a representative elevation. Replacing the mean temperature with mean catchment elevation, a very good proxy for average temperature, the expected strong relationship with z^* becomes visible (Figure 10). This plot, however, also shows that the method probably fails to give a reliable estimate of the responsive area for the Riale de Calneggia, which falls far away from the regression line for all other case studies.

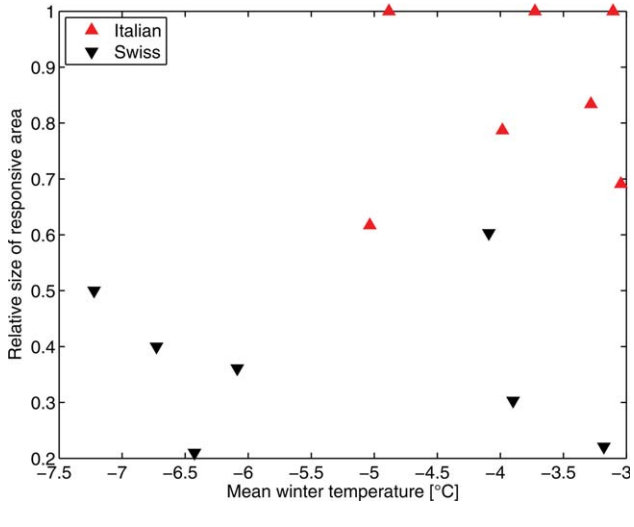

Figure 9. Relation between the mean winter temperature and the relative size of the responsive area for the Swiss and the Italian catchments.

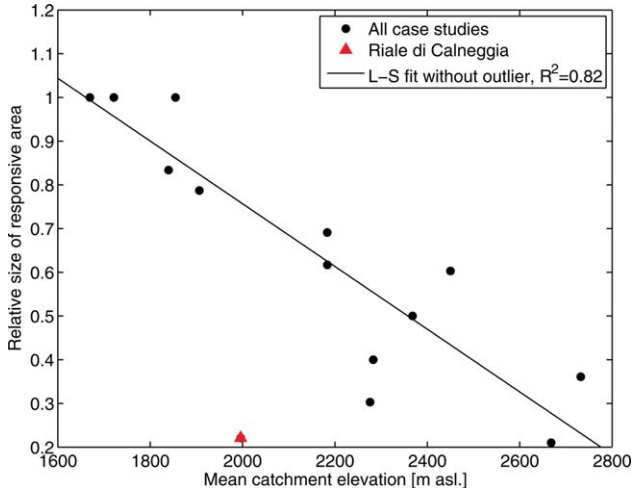

Figure 10. Linear relation between the mean catchment elevation and the relative size of the responsive area for all case studies; the least-square (L-S) regression line is fitted to all points except the outlier Riale di Calneggia.

[53] Two hypotheses can be advanced: either the estimated average precipitation is far too high, leading to a very small responsive area or the observed winter streamflow is considerably underestimated. Riale di Calneggia shows much higher average precipitation on wet days than the other catchments; this is, however, plausible in this area of the Alps, which has relatively high-annual precipitation amounts [*Schwarb et al*., 2001]. The hypothesis of erroneous winter discharge observations cannot be rejected, especially because this mountainous torrent has no well defined low-flow channel at the outlet.

5. Discussion

[54] The presented analytic streamflow pdf describes the winter hydrologic response of snow-dominated catchments based on five parameters which can easily be estimated from observed precipitation ($\alpha, \gamma'_P, \lambda_P$), temperature ($\tau_D$) and discharge ($\tau_k$) and one calibration parameter (z^*) which incorporates indirectly additional temperature effects on the winter flow distribution and which has been shown in this paper to have a strong relation to mean catchment altitude. In this respect, it is important to keep in mind the limitations of the proposed approach and of the direct physical interpretation of the model parameters. Some of the model parameters depend on the selected observation periods. This might a priori have an important impact on the mean observed streamflow (and thus on the calibrated z^*), in particular if the selected period is too short to observe the release of all the incoming precipitation from the contributing part of the catchment. For the selected case studies, the value of τ_w varies between 15 and 63 days, which is a strong hint that the selected period (December-February) is long enough. Further analyses are necessary to refine the definition of the winter season if the model was to be applied to catchments with much higher mean elevations (implying much longer winters) or with a different climate (where there might not exist a season corresponding to the alpine winter, see e.g., the climates studied by *Kaser et al*. [2010]).

[55] Observational uncertainties might affect all estimated model parameters. Questions related to the nonrepresentativity of the reference meteorological time series have been discussed earlier in this paper (section 4.1). For streamflow, observational errors [*Westerberg et al*., 2011] are likely to occur during winter low flow due to freezing of the measurement devices or of the river itself. Such measurement errors might influence the value of z^*, given that it is calibrated on average winter low flow. How to properly estimate the effect of observational uncertainties on the model parameters is left for future research.

[56] A strong impact on the estimated parameter values might also be expected from the time variability of the stream network activation. The residence time parameter τ_k is estimated for the summer period when the entire stream network is participating in the hydrological response and it is subsequently used to model winter streamflow. We might expect, therefore, that τ_k overestimates the snow-free residence time of the (smaller) responsive catchment part during the winter. However, for the kind of steep environments that are studied in this paper, this effect is likely to be negligible.

[57] Overall, the proposed novel method condenses into one partition parameter (z^*) most uncertainties of the hydrologic response, which is remarkable given the complexity of high-mountainous systems.

6. Conclusions

[58] The analytic model for winter low flow proposed in this paper is an extension over the analytic model of *Botter et al*. [2007b] for catchments that experience significant snowfall but that are still responsive during winter. The model has been successfully applied to a range of catchments in the Swiss and the Italian Alps. The good model performance along with the plausible regional behavior of the calibrated model parameter suggests that knowledge about topography and the climate might be sufficient to determine winter streamflow distributions for Alpine catchments with nival regimes. The applicability of the proposed method to other climatic regions [e.g., *Thayyen and Gergan*, 2010; *Kaser et al*., 2010] remains to be tested; it namely depends on the existence of a pronounced winter low-flow period which results from temporal precipitation storage in the snowpack without significant seasonal carryover or groundwater inflow.

[59] The interest of this approach is twofold: On one hand, the case studies suggested that there is a strong dependence of the model parameter that identifies the responsive area (z^*) on mean catchment elevation; this points toward a high potential for spatial and temporal transferability of the model to estimate winter streamflow in ungauged catchments or for evolving climates. Such regionalized winter streamflow pdfs could also contribute to the calibration of rainfall-runoff models based on flow-duration curves, which tends to fail for snow-influenced catchments [*Westerberg et al*., 2011].

[60] On the other hand, the proposed approach infers the average responsive catchment area from observed streamflow, i.e., the analytic streamflow pdf represents a means to

explicitly extract information about snow dynamics from observed streamflow. Even if such information oversimplifies the very complex distribution of snow [e.g., *Blöschl*, 1999; *Lehning et al*., 2011; *Egli et al*., 2012], this might nevertheless open new perspectives for the development of snow hydrological models where direct information about the snow cover is lacking and has to be modeled from precipitation observations alone (which is highly error-prone, see *Grünewald and Lehning* [2011]).

[61] We conclude that the proposed method contributes to bridge a gap existing in the hydrological literature in the determination of streamflow distributions (and hence discharge duration curves) for cases where seasonal snow/rain partitioning is a factor. Implications for quantitative water resources management and ecohydrological functions that rely on streamflow fluctuations [*Doyle et al*., 2005] are deemed notable.

[62] **Acknowledgments.** The research of the first author was supported by a research grant of the Swiss National Science Foundation (SNF, PZ00P2_126607). Funds provided to the second author by the ERC advanced grant program through the project RINEC-227612 and by the SFN/FNS project 200021 124930/1 are gratefully acknowledged. The third author acknowledges funding from the research grant "Progetto di Ateneo 2010" (CPDA105501/10). The authors also thank Federico De Piccoli for his help in analyzing the data and testing the model. For the Piave river, all observed data were provided by the Regional Agency for the Environment of Veneto (ARPAV, www.arpa.veneto.it). The meteorological data for the Swiss case studies were provided by MeteoSwiss (www.meteoswiss.ch) and the discharge data by the Swiss Federal Office for the Environment (2009, www.bafu.admin.ch/hydrologie).

References

Allamano, P., P. Claps, and F. Laio (2009), Global warming increases flood risk in mountainous areas, *Geophys. Res. Lett.*, *36*, L24404, doi:10.1029/2009gl041395.

Bayard, D., M. Stähli, A. Parriaux, and H. Flühler (2005), The influence of seasonally frozen soil on the snowmelt runoff at two Alpine sites in southern Switzerland. *J. Hydrol.*, *309*(1–4), 66–84, doi:10.1016/j.jhydrol.2004.11.012.

Blöschl, G. (1999), Scaling issues in snow hydrology, *Hydrol. Process.*, *13*(14–15), 2149–2175.

Botter, G. (2010) Stochastic recession rates and the probabilistic structure of stream flows, *Water Resour. Res.*, *46*, W12527, doi:10.1029/2010WR009217.

Botter, G., F. Peratoner, A. Porporato, I. Rodriguez-Iturbe, and A. Rinaldo (2007a), Signatures of large-scale soil moisture dynamics on streamflow statistics across US climate regimes, *Water Resour. Res.*, *43*, W11413, doi:10.1029/2007wr006162.

Botter, G., A. Porporato, I. Rodriguez-Iturbe, and A. Rinaldo (2007b), Basin-scale soil moisture dynamics and the probabilistic characterization of carrier hydrologic flows: Slow, leaching-prone components of the hydrologic response, *Water Resour. Res.*, *43*, W02417, doi:10.1029/2006wr005043.

Botter, G., S. Zanardo, A. Porporato, I. Rodriguez-Iturbe, and A. Rinaldo (2008), Ecohydrological model of flow duration curves and annual minima, *Water Resour. Res.*, *44*, W08418, doi:10.1029/2008wr006814.

Botter, G., S. Basso, A. Porporato, I. Rodriguez-Iturbe, and A. Rinaldo (2010), Natural streamflow regime alterations: Damming of the Piave river basin (Italy), *Water Resour. Res.*, *46*, W06522, doi:10.1029/2009wr008523.

Bourgouin, P. (2000), A method to determine precipitation types, *Weather Forecasting*, *15*(5), 583–592, doi:10.1175/1520-0434(2000)015¡0583:amtdpt¿2.0.co;2.

Brutsaert, W., and J. L. Nieber (1977), Regionalized drought flow hydrographs from a mature glaciated plateau, *Water Resour. Res.*, *13*(3), 637–644, doi:10.1029/WR013i003p00637.

Ceola, S., G. Botter, E. Bertuzzo, A. Porporato, I. Rodriguez-Iturbe, and A. Rinaldo (2010), Comparative study of ecohydrological streamflow probability distributions. *Water Resour. Res.*, *46*, W09502, doi:10.1029/2010wr009102.

Clark, M. P., J. Hendrikx, A. G. Slater, D. Kavetski, B. Anderson, N. J. Cullen, T. Kerr, E. O. Hreinsson, and R. A. Woods (2011), Representing spatial variability of snow water equivalent in hydrologic and land-surface models: A review, *Water Resour. Res.*, *47*, W07539 doi:10.1029/2011wr010745.

DeBeer, C. M., and J. W. Pomeroy (2010), Simulation of the snowmelt runoff contributing area in a small alpine basin, *Hydrol. Earth Syst. Sci.*, *14*(7), 1205–1219, doi:10.5194/hess-14–1205-2010.

Doyle, M. W., E. Stanley, D. Strayer, R. Jacobson, and J. Schmidt (2005), Effective discharge analysis of ecological processes in streams, *Water Resour. Res.*, *41*, W11411, doi:10.1029/2005WR004222.

Egli, L., T. Jonas, T. Grünewald, M. Schirmer, and P. Burlando (2012), Dynamics of snow ablation in a small Alpine catchment observed by repeated terrestrial laser scans, *Hydrol. Process.*, *26*(10), 1574–1585, doi:10.1002/hyp.8244.

Grünewald, T., and M. Lehning (2011), Altitudinal dependency of snow amounts in two small Alpine catchments: Can catchment-wide snow amounts be estimated via single snow or precipitation stations? *Ann. Glaciol.*, *52*(58), 153–158, doi:10.3189/172756411797252248.

Grünewald, T., M. Schirmer, R. Mott, and M. Lehning (2010), Spatial and temporal variability of snow depth and ablation rates in a small mountain catchment, *Cryosphere*, *4*(2), 215–225, doi:10.5194/tc-4–215-2010.

H. S. Swiss Federal Office for the Environment (2009), *Hydrologisches Jahrbuch der Schweiz*, Swiss Fed. Off. for the Environ. (FOEN), Bern.

Hannah, D. M., S. R. Kansakar, A. J. Gerrard, and G. Rees (2005), Flow regimes of Himalayan rivers of Nepal: Nature and spatial patterns, *J. Hydrol*, *308*(14), 18–32, doi:10.1016/j.jhydrol.2004.10.018.

Hantel, M., and L.-M. Hirtl-Wielke (2007), Sensitivity of Alpine snow cover to European temperature, *Int. J. Climatol.*, *27*(10), 1265–1275, doi: 10.1002/joc.1472.

Hock, R. (2003), Temperature index melt modelling in mountain areas, *J. Hydrol.*, *282*(1–4), 104–115, doi:10.1016/S0022–1694(03)00257-9.

Horton, P., B. Schaefli, B. Hingray, A. Mezghani, and A. Musy (2006), Assessment of climate change impacts on Alpine discharge regimes with climate model uncertainty, *Hydrol. Process.*, *20*, 2091–2109.

Jabot, E., I. Zin, T. Lebel, A. Gautheron, and C. Obled (2012), Spatial interpolation of sub-daily air temperatures for snow and hydrologic applications in mesoscale Alpine catchments, *Hydrol. Process.*, *26*(17), 2618–2630, doi: 10.1002/hyp.9423.

Kaser, G., M. Grosshauser, and B. Marzeion (2010), Contribution potential of glaciers to water availability in different climate regimes, *PNAS*, *107*(47), 20,223–20,227, doi:10.1073/pnas.1008162107.

Laio, F., A. Porporato, L. Ridolfi, and I. Rodriguez-Iturbe (2001), Plants in water-controlled ecosystems: Active role in hydrologic processes and response to water stress—ii. Probabilistic soil moisture dynamics, *Adv. Water Resour.*, *24*(7), 707–723, doi:10.1016/s0309–1708(01)00005–7.

Lehmann, E. L., and J. P. Romano (2005), *Testing Statistical Hypotheses*, Springer, New York.

Lehning, M., I. Völksch, D. Gustafsson, T. A. Nguyen, M. Stähli, and M. Zappa (2006), ALPINE3D: A detailed model of mountain surface processes and its application to snow hydrology, *Hydrol. Process.*, *20*(10), 2111–2128, doi:10.1002/hyp.6204.

Lehning, M., T. Grunewald, and M. Schirmer (2011), Mountain snow distribution governed by an altitudinal gradient and terrain roughness, *Geophys. Res. Lett.*, *38*, L19504, doi:10.1029/2011gl048927.

Magnusson, J., D. Farinotti, T. Jonas, and M. Bavay (2011), Quantitative evaluation of different hydrological modelling approaches in a partly glacierized swiss watershed, *Hydrol. Process.*, *25*(13), 2071–2084, doi: 10.1002/hyp.7958.

Marks, D., J. Kimball, D. Tingey, and T. Link (1998), The sensitivity of snowmelt processes to climate conditions and forest cover during rain-on-snow: A case study of the 1996 Pacific Northwest flood, *Hydrol. Process.*, *12*(10–11), 1569–1587, doi:10.1002/(sici)1099-1085(199808/09)12: 10/11¡1569::aid-hyp682¿3.0.co;2-l.

Molini, A., G. G. Katul, and A. Porporato (2011), Maximum discharge from snowmelt in a changing climate, *Geophys. Res. Lett.*, *38*(5), L05402, doi: 10.1029/2010gl046477.

Ohmura, A. (2001), Physical basis for the temperature-based melt-index method, *J. Appl. Meteorol.*, *40*(4), 753–761.

Perona, P., A. Porporato, and L. Ridolfi (2007), A stochastic process for the interannual snow storage and melting dynamics, *J. Geophys. Res.*, *112*, D08107, doi:10.1029/2006jd007798.

Perona, P., N. Pasquale, and D. Molnar (2008), Mechanistic interpretation of Alpine glacierized environments: Part 2. Hydrologic interpretation

and model parameters identification on case study, *Adv. Water Resour.*, *31*(7), 948–961, doi:10.1016/j.advwatres.2008.03.007.

Rodriguez-Iturbe, I., and A. Porporato (2004), *Ecohydrology of Water-Controlled Ecosystems—Soil Moisture and Plant Dynamics*, Cambridge Univ. Press, Cambridge.

Rodriguez-Iturbe, I., V. K. Gupta, and E. Waymire (1984), Scale considerations in the modelling of temporal rainfall, *Water Resour. Res.*, *20*(11), 1611–1619, doi:10.1029/WR020i011p01611.

Rodriguez-Iturbe, I., A. Porporato, L. Ridolfi, V. Isham, and D. Cox (1999), Probabilistic modelling of water balance at a point: The role of climate, soil and vegetation, *Proc. R. Soc. London A*, *455*, 3789–3805.

Rohrer, M. B., L. N. Braun, and H. Lang (1994), Long-term records of snow cover water equivalent in the swiss Alps. 1. analysis, *Nordic Hydrol.*, *25*(1–2), 53–64.

Schaefli, B., B. Hingray, M. Niggli, and A. Musy (2005), A conceptual glacio-hydrological model for high mountainous catchments, *Hydrol. Earth Syst. Sci.*, *9*, 95–109, doi:10.5194/hessd-2–73-2005.

Schwarb, M., C. Daly, C. Frei, and C. Schär (2001), Mean annual precipitation throughout the European Alps, 1971–1990, Hydrological atlas of Switzerland, plate 2.6, *Swiss Nat. Hydrol. and Geol. Surv., Berne.* [Available at http://hades.unibe.ch, accessed 15 Apr 2013.].

Settin, T., G. Botter, I. Rodriguez-Iturbe, and A. Rinaldo (2007), Numerical studies on soil moisture distributions in heterogeneous catchments, *Water Resour. Res.*, *43*, W05425, doi:10.1029/2006wr005737.

Sevruk, B. (1997), Regional dependency of precipitation-altitude relationship in the Swiss Alps, *Clim. Change*, *36*, 255–369, doi:10.1023/A:1005302626066.

Stahl, K., R. Moore, J. Shea, D. Hutchinson, and A. Cannon (2008), Coupled modelling of glacier and streamflow response to future climate scenarios, *Water Resour. Res.*, *44*, W02422, doi:10.1029/2007WR005956.

Suter, S., T. Konzelmann, C. Mühlhäuser, M. Begert, and A. Heimo (2006), SWISSMETNET the new automatic meteorological network of Switzerland: Transition from old to new network, *data management and first results*, Tech. Rep. [Available at http://www.meteoschweiz.admin.ch/web/, accessed 16 Apr. 2013.].

SwissTopo (2005), *DHM25—The Digital Height Model of Switzerland*, Federal Office of Topography, Bern, Switzerland.

SwissTopo (2008), *Vector25—The Digital Landscape Model of Switzerland*, Federal Office of Topography, Bern, Switzerland.

Thayyen, R. J., and J. T. Gergan (2010), Role of glaciers in watershed hydrology: A preliminary study of a Himalayan catchment, *Cryosphere*, *4*(1), 115–128, doi:10.5194/tc-4–115-2010.

The Geocommunity (2013), Italy—Nationwide data. [Available at http://data.geocomm.com/. 2013, accessed 31 Jan. 2013.].

Tobin, C., L. Nicotina, M. B. Parlange, A. Berne, and A. Rinaldo (2011), Improved interpolation of meteorological forcings for hydrologic applications in a Swiss Alpine region, *J. Hydrol.*, *401*(1–2), 77–89, doi:10.1016/j.jhydrol.2011.02.010.

Tobin, C., A. Rinaldo, and B. Schaefli (2012), Snowfall limit forecasts and hydrological modeling, *J. Hydrometeorol.*, *13*(5),1507–1519, doi:10.1175/JHM-D-11–0147.1.

Tobin, C., B. Schaefli, L. Nicótina, S. Simoni, G. Barrenetxeae, R. Smith, M. Parlange, and A. Rinaldo (2013), Improving the degree-day method for sub-daily melt simulations with physically-based diurnal variations, *Adv. Water Resour.*, doi:10.1016/j.advwatres.2012.08.008, in press.

Viviroli, D., and R. Weingartner (2004), The hydrological significance of mountains: From regional to global scale, *Hydrol. Earth Syst. Sci.*, *8*(6), 1017–1030, doi:10.5194/hess-8-1017-2004.

Westerberg, I. K., J. L. Guerrero, P. M. Younger, K. J. Beven, J. Seibert, S. Halldin, J. E. Freer, and C. Y. Xu (2011), Calibration of hydrological models using flow-duration curves. *Hydrol. Earth Syst. Sci.*, *15*(7), 2205–2227, doi:10.5194/hess-15–2205-2011.

Woods, R. A. (2009), Analytical model of seasonal climate impacts on snow hydrology: Continuous snowpacks, *Adv. Water Resour.*, *32*(10), 1465–1481, doi:10.1016/j.advwatres.2009.06.011.

Woody, J., R. Lund, A. J. Grundstein, and T. L. Mote (2009), A storage model approach to the assessment of snow depth trends, *Water Resour. Res.*, *45*, W10426, doi:10.1029/2009wr007996.

Zappa, M., F. Pos, U. Strasser, P. Warmerdam, and J. Gurtz (2003), Seasonal water balance of an alpine catchment as evaluated by different methods for spatially distributed snowmelt modelling, *Nordic Hydrol.*, *34*(3), 179–202.